

HMSIW Tri-Band Filtering Power Divider

Xu Wang*, Ling-Qin Meng, Wei Wang, and Dan-Dan Lv

Abstract—A tri-band two-way filtering power divider structure is proposed based on HMSIW. Dual-band filtering power divider is realized by etching semicircular slots on HMSIW. The third passband is achieved by loading open-stub without affecting two other passbands. The return loss is less than -20 dB in each passband with 3 dB fractional bandwidths of 3.75%, 9.3% and 0.61%. The measured results are in agreement with the simulated ones in this paper. This filtering power divider has the advantages of simple structure, easy integration, etc. It has a good application prospect.

1. INTRODUCTION

With the development of microwave and millimeter wave technology, modern communication system has raised requirements higher and higher for the circuit size. So the integration and miniaturization have been the hot areas of research in recent years. Filter and power divider are important components in microwave communication system [1]. It is proposed that filter and power divider are integrated in the process of pursuing miniaturization [2]. Filtering power divider can not only reduce the size of circuit and insertion loss, but also reduce costs [3]. A lot of filtering power divider research is based on microstrip structure [4–6]. The structure is easy to integrate, but it has low quality and low-power capability. Meanwhile, the insertion loss becomes larger with the increase of frequency. The transmission characteristics of the substrate integrated waveguide (SIW) are similar to the rectangular waveguide. So the substrate integrated waveguide is widely used in the design of various microwave passive devices such as filter, power divider and other microwave passive devices. The concept of half-mode substrate integrated waveguide (HMSIW) is presented in [7]. Compared to SIW, the size of HMSIW decreases about 50%. Some filtering power dividers based on SIW have been studied in recent years [8–11]. SIW power divider loading complementary split ring resonator (CSRR) or defected ground structure (DGS) to achieve bandpass is commonly used by scholars. However, the research in SIW filtering power divider is mainly focused on broadband, high isolation, etc. At present, there is little research on dual-band or multiband SIW filtering power divider.

In order to obtain multiband filtering power divider with small size, high quality factor and large transmission power, a tri-band filtering power divider by etching semicircular slots on an HMSIW T-junction power divider and loading open-stub is designed and fabricated. First, a dual-band filter power divider is designed by analyzing the radius of the etched semicircle slots, width of slots and spacing between the inner and outer slots. Then, an open-stub is loaded on the dual-band filtering power divider to achieve the third passband. The filtering power divider has triple passbands center frequencies of 4.53 GHz, 6.53 GHz, and 8.32 GHz.

Received 11 March 2017, Accepted 27 April 2017, Scheduled 14 May 2017

* Corresponding author: Xu Wang (wangxuedu@163.com).

The authors are with the Key Laboratory of Specialty Fiber Optics Access Network, Shanghai University, Shanghai 200072, China.

2. ANALYSIS AND DESIGN OF HMSIW FILTERING POWER DIVIDER

2.1. Design of Dual-Band Filtering Power Divider

The SIW can be regarded as a pair of transmission lines. The upper and lower metal layers are connected by metallic vias resulting in short stubs. SIW has the same transmission characteristics as rectangular waveguide. In SIW structure, only TE_{n0} mode can propagate, and the dominant mode of SIW is TE_{10} . The cutoff frequency of the SIW can be calculated by the following formula [12].

$$f_{TE_{10}} = \frac{c_0}{2W_{eff}\sqrt{\epsilon_r}} \quad (1)$$

The resonant frequency of TE_{m0n} can be calculated by the following formula [13].

$$f_{TE_{m0n}} = \frac{c_0}{2\sqrt{\epsilon_r}} \sqrt{\left(\frac{m}{w_{eff}}\right)^2 + \left(\frac{n}{l_{eff}}\right)^2} \quad (2)$$

From formula (2), frequency ratio can be obtained: $f_{TE_{102}}/f_{TE_{101}} \approx 1.58$. When TE_{101} and TE_{102} are perturbed to different degrees, the ratio will change.

The half mode substrate integrated waveguide (HMSIW) has the same transmission characteristics as SIW. The dominant mode of HMSIW is TE_{10} . The cutoff frequency of the SIW can be calculated by the following formula:

$$f_{TE_{10}} = \frac{c_0}{4W_{HMSIW_{eff}}\sqrt{\epsilon_r}} \quad (3)$$

In Equations (1), (2), (3) and (4), w_{eff} is the equivalent width of SIW, l_{eff} the equivalent length of SIW, c_0 the light velocity in vacuum, ϵ_r the relative permittivity of the substrate, $W_{HMSIW_{eff}}$ the equivalent width of HMSIW.

To achieve the cutoff frequency of HMSIW, the highpass characteristic of HMSIW is analyzed by simulation. The whole work is based on full wave software Ansoft HFSS. A 0.508 mm thick Rogers RO4350B is used in this paper with a relative permittivity of 3.48, and dielectric loss tangent of 0.0037. $L_{siw} = 18$ mm, $W_{siw} = 8.9$ mm. The simulated results of cutoff frequency is shown in Fig. 1(b). The cutoff frequency is 4.3 GHz. The return loss is less than -15 dB, and the maximum insertion loss is 0.92 dB in passband.

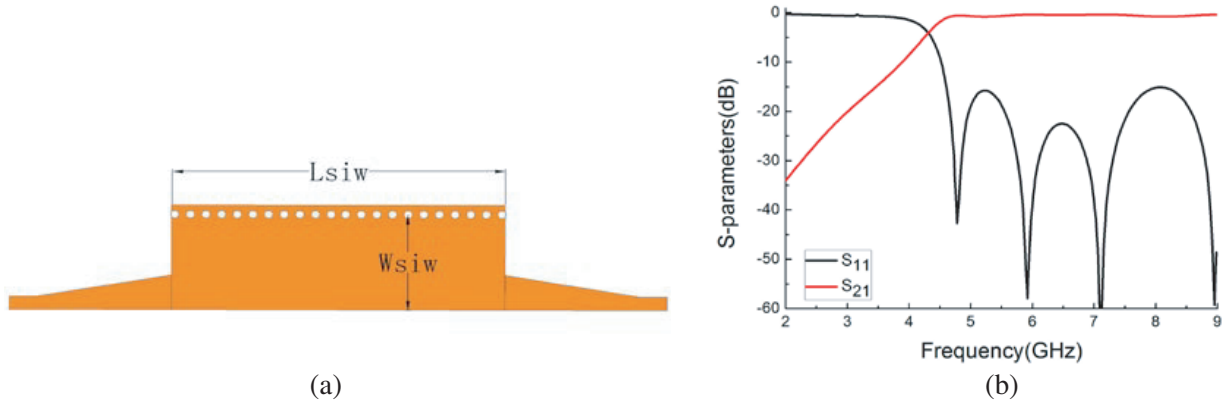


Figure 1. (a) The structure of HMSIW. (b) The simulated S -parameters of HMSIW.

The substrate integrated waveguide T power divider is symmetrical, which is used in the design of 3 dB power divider. The outputs have good amplitude and phase performance. The structure of HMSIW T power divider is shown in Figure 2(a). Port1 is the input with coplanar waveguide (CPW). Port2 and Port3 are the outputs with SIW to microstrip line transition. The dominant mode of HMSIW transmission is TE_{10} mode. The first passband operates in the state of the first mode TE_{101} . When L_s is 48 mm, the relation between the first center frequency and W_s is shown in Figure 2(b).

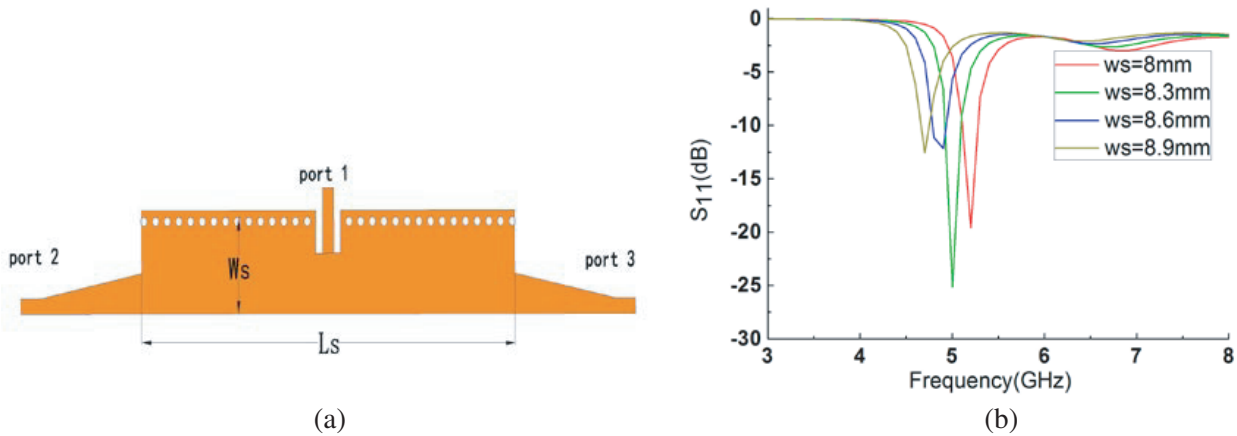


Figure 2. (a) Structure of T type power divider. (b) The simulated return loss under different values of W_s .

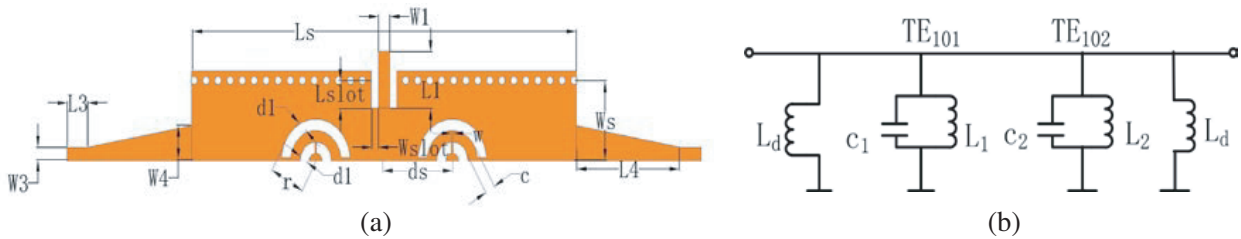


Figure 3. (a) The structure of the power divider filter. (b) The equivalent circuit of the resonant elements.

Because the electric field is perpendicular to the metal surfaces in HMSIW, the TE_{102} mode can be excited by semicircle ring slots etched on HMSIW cavity. A new resonant element is created when the slots are etched at the symmetrical position of the cavity. The circuit structure and equivalent circuit are shown in Figures 3(a) and (b). In Figure 3(a), the outer radius of the semicircular slot is r ; the width of the slots is $d1$; the distance between slots is c . In Figure 3(b), the first center frequency f_1 (TE_{101}) is represented by C_1 and L_1 ; the second center frequency f_2 (TE_{102}) is represented by C_2 and L_2 .

Thus, a dual-band filtering divider can be achieved by loading slots on the HMSIW cavity. The resonator is excited by the slots, so the resonance frequency is affected by the HMSIW width W_s , outer radius r , slots width $d1$, and distance c between the slots. f_2 (TE_{102}) is about 1.5 times of f_1 (TE_{101}). When $d1$ and c are fixed, f_1 and f_2 will change with r . When r increases, the size of the slots increases, and the distribution of the (TE_{101} and TE_{102}) current on the HMSIW changes. As shown in Figure 4(a), f_1 and f_2 move to lower frequency. According to [14] and simulation results, the approximate relation between f_2 and r is obtained:

$$\pi r \approx \frac{1}{4} \lambda_{g2} \tag{4}$$

where λ_{g2} is the guide wavelength of the centre frequency of the second passband. When r and c are fixed and the value of $d1$ increases, the inductive coupling and capacitive coupling of the slots decrease. The corresponding L_1 , L_2 , C_1 and C_2 decrease, f_1 and f_2 move to higher frequency, shown in Figure 4(b). When r and $d1$ are fixed and the value of c increases, the corresponding capacitance C_2 and inductance L_2 decrease, but the current distribution of TE_{101} mode is hardly affected. So f_2 moves to lower frequency, and f_1 dose not change, shown in Figure 4(c). When only the value of W_s decreases, the cutoff frequency moves to lower frequency, and f_1 and f_2 also move to lower frequency.

A dual-band filtering power divider is designed based on the relation that f_2 (TE_{102}) is about 1.5 times of f_1 (TE_{101}). The dual-band filtering power divider is simulated in Ansoft HFSS based

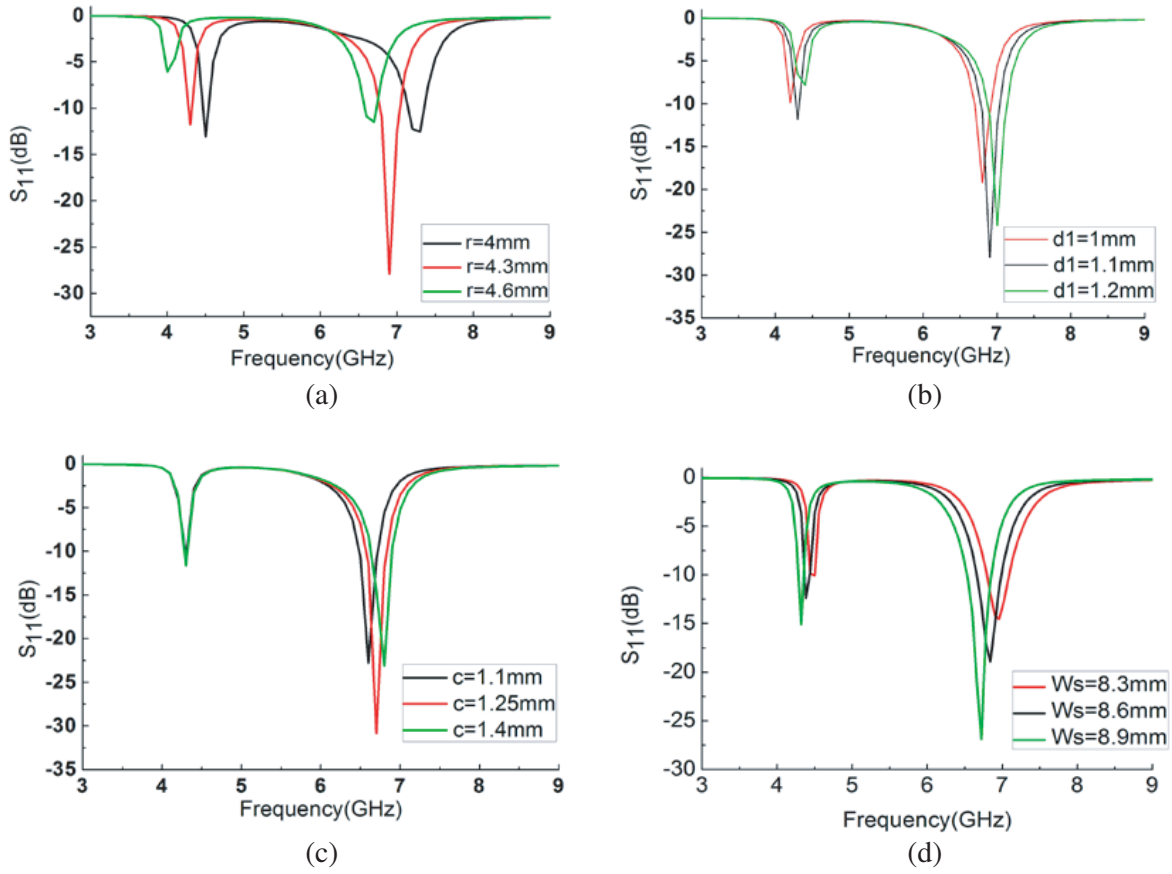


Figure 4. (a) The simulated return loss under different values of r . (b) The simulated return loss under different values of $d1$. (c) The simulated return loss under different values of c . (d) The simulated return loss under different values of W_s .

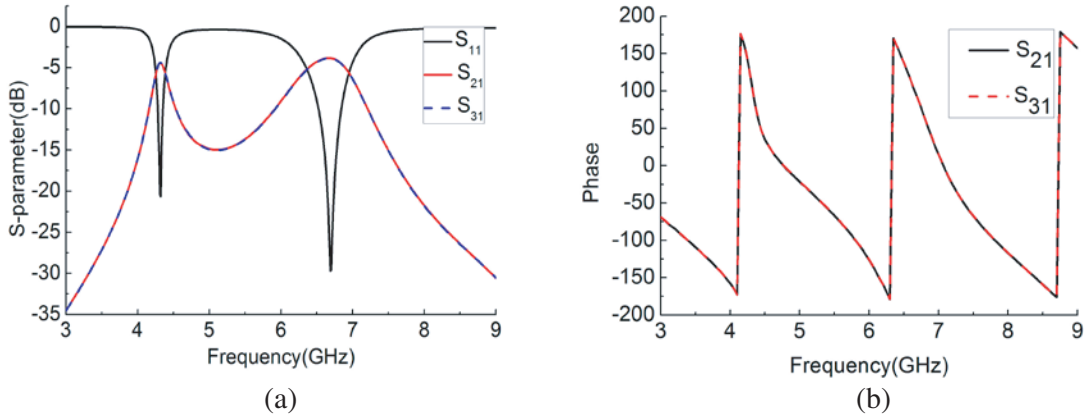


Figure 5. (a) The simulated results of dual-band filtering power divider. (b) Simulated phase response of the dual-band filtering power divider.

on Rogers RO4350B, and the parameters are obtained. $L_s = 48\text{ mm}$, $W_s = 8.6\text{ mm}$, $L_1 = 5.84\text{ mm}$, $W_1 = 1.42\text{ mm}$, $L_{\text{slot}} = 2.84\text{ mm}$, $W_{\text{slot}} = 0.88\text{ mm}$, $L_3 = 2.54\text{ mm}$, $W_3 = 1.39\text{ mm}$, $L_4 = 13\text{ mm}$, $W_4 = 3.63\text{ mm}$, $W = 0.33$, $r = 4.3\text{ mm}$, $c = 1.2\text{ mm}$, $d1 = 1.16\text{ mm}$, $d_s = 8\text{ mm}$. The results of simulation are shown in Figure 5. The return losses of the dual-band filtering power divider at 4.45 GHz

and 6.6 GHz are below -20 dB, and the minimum insertion losses at 4.45 GHz and 6.6 GHz are -4.2 dB and -3.4 dB, respectively. The output ports have the same phase and amplitude.

2.2. Design of Tri-Band Filter Power Divider

An open-stub structure is shown in Figure 6(a), where Y_1 , h_1 , Y_2 and h_2 denote the characteristic admittances and lengths of the microstrip line, respectively. An HMSIW structure has no effect on even modes, whereas odd modes are no longer excited. For even-mode excitation, we can bisect the circuit with open circuits at the middle to obtain the equivalent circuit of Figure 6(b). At the even-mode resonant frequencies, the lengths of the microstrip line is [15]:

$$\theta_2 + \theta_1/2 = n\pi, \quad n = 1, 2, 3, \dots, \quad \text{or} \quad h_2 + h_1/2 = \frac{n\lambda_g}{2}, \quad n = 1, 2, 3, \dots \quad (5)$$

where λ_g is the guided wavelength at even-mode resonance, and Θ_1 and Θ_2 are the electric lengths of h_1 and h_2 .

A tri-band filtering power divider is obtained by loading open-stub based on dual-band filtering power divider. The open-stub is at the center of HMSIW, and it is symmetrical as shown in Figure 7. When the open-stub is at resonance state, the positions of the other two resonant frequencies are not affected. The circuit has the advantages of simple structure, low cost, easy integration, etc.

According to the theoretical analysis, the third resonant frequency is related to L_5 , L_6 and L_7 in Figure 7. When the value of L_5 increases, f_3 moves to lower frequency. Meanwhile, the first and second center frequencies are not changed, as shown in Figure 8(a). The tri-band filtering power divider is designed and simulated in Ansoft HFSS, and the parameters of the design are obtained. $L_s = 48$ mm, $W_s = 8.6$ mm, $L_1 = 5.8$ mm, $W_1 = 1.4$ mm, $L_{slot} = 2.8$ mm, $W_{slot} = 0.9$ mm, $L_3 = 2.54$ mm, $W_3 = 1.38$ mm, $L_4 = 13$ mm, $W_4 = 3.6$ mm, $L_5 = 4.5$ mm, $W_5 = 1.2$ mm, $L_6 = 19.15$ mm, $W_6 = 1$ mm, $L_7 = 2$ mm, $D = 0.8$ mm, $dv = 1.5$ mm, $ds = 8$ mm, $r = 4.3$ mm, $d1 = 1.1$ mm, $c = 1.26$ mm. Figure 8(b) shows the simulated results of tri-band filtering power divider.

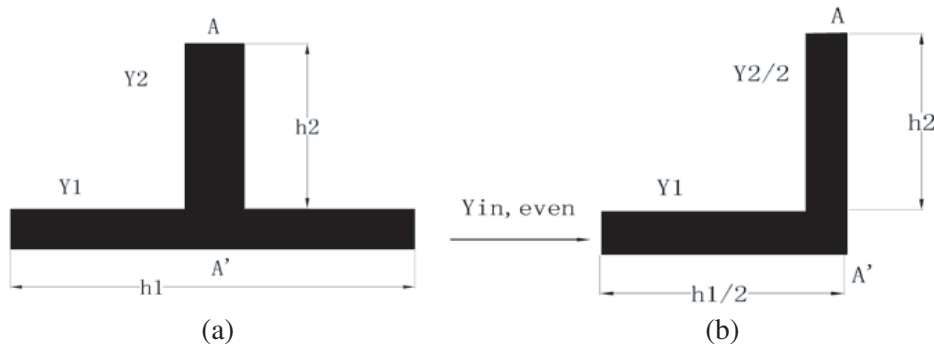


Figure 6. (a) Structure of the open-stub resonator. (b) Even-mode equivalent circuit.

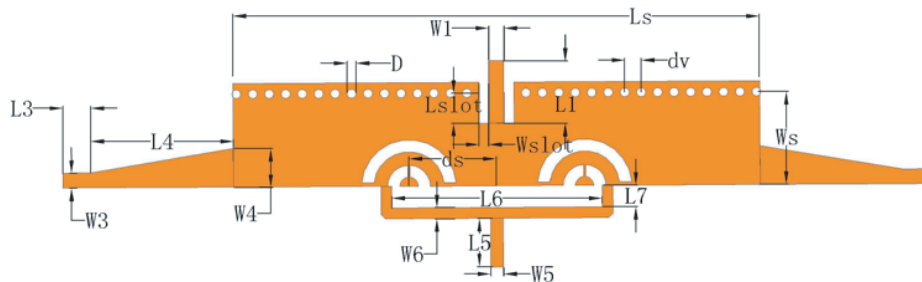


Figure 7. The structure of tri-band filtering power divider.

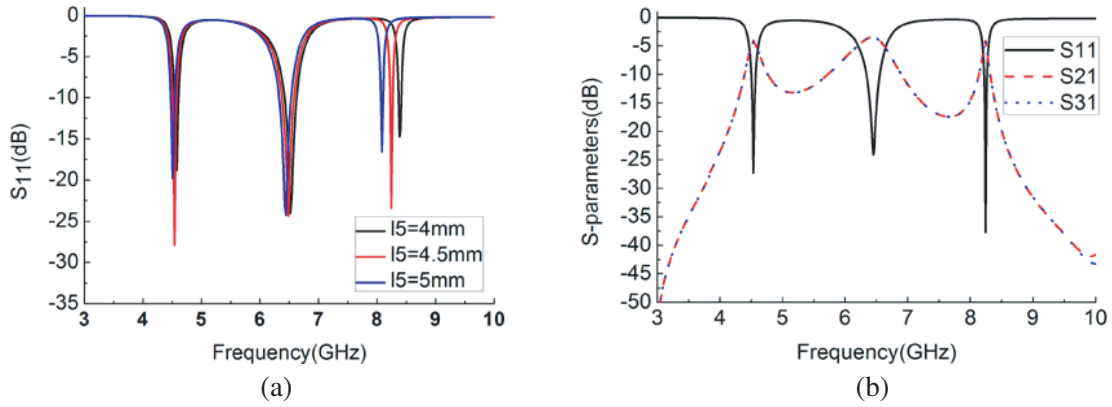


Figure 8. (a) The simulated return loss under different values of L_5 . (b) The simulated results of tri-band filtering power divider.

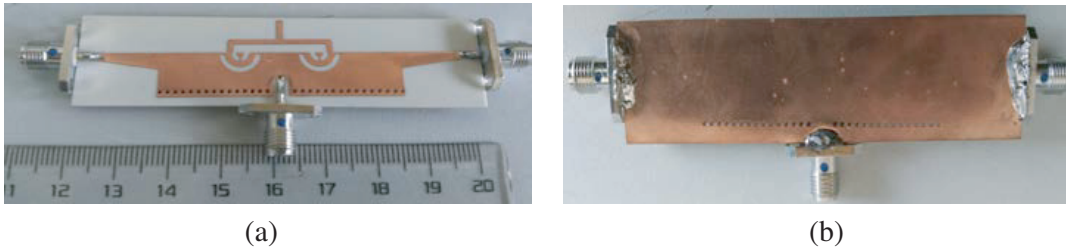


Figure 9. The photograph of the fabricated filtering power divider.

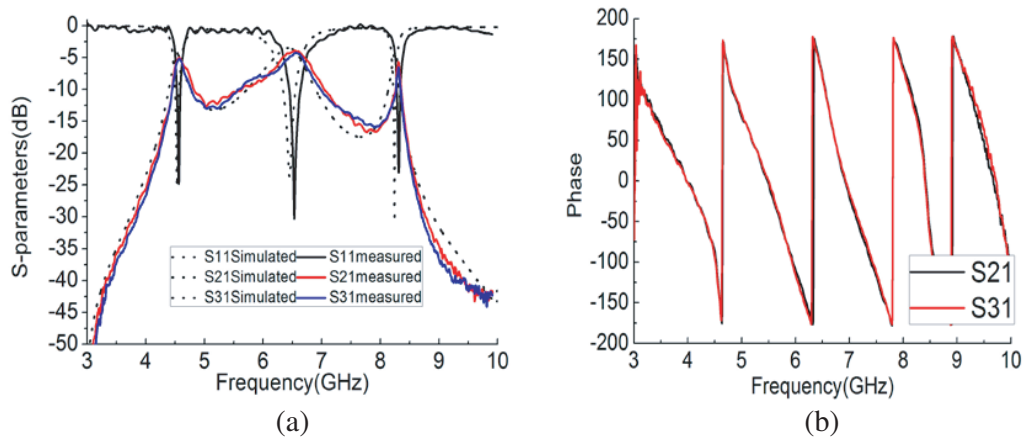


Figure 10. (a) Measured and simulated S_{11} , S_{21} and S_{31} . (b) Measured phase response of the proposed power divider.

3. FABRICATION AND EXPERIMENT

The power divider is fabricated on a 0.508 mm thick Rogers RO4350B with a relative permittivity 3.48 and dielectric loss tangent of 0.0037. Photographs of the proposed power divider are shown in Figure 9. The fabricated filtering power divider is measured using Agilent 8722ES network analyzer. Figure 10 indicates the simulated and measured results.

It is shown in Figure 10(a) that the measured resonant frequencies of the filtering power divider appear at 4.53 GHz, 6.53 GHz, 8.32 GHz with return losses of -24 dB, -30 dB, -22 dB and the minimum

insertion losses of -4.6 dB, -4.1 dB, -5.1 dB, respectively. The measured 3 dB fractional bandwidth is 3.75%, 9.3% and 0.61%. The simulated and measured results are in good agreement. There is a slight shift at the second and third resonant frequencies. Due to the SMA connector loss, fabrication tolerance, measurement error, etc., the measured results are slightly worse than the simulated ones. Figure 10(b) depicts the measured phase response of the proposed filtering power divider. It can be seen that the proposed power divider has a good phase performance within the passband.

In Table 1, a comparison between this work and other tri-band power dividers is summarized. In this table, the advantage in frequency response is obvious. Furthermore, the proposed filtering power divider is based on HMSIW, which has higher Q -factor than that in [16–20].

Table 1. Comparison with other tri-band power dividers.

Reference	Frequency (GHz)	Insertion loss (dB)	Frequency Response	Topology
[16]	0.92/2.45/5.8	3.2/3.5/4.1	No	Microstrip line
[17]	0.93/2.3/3.6	4.56/4.35/4.25	No	Microstrip line
[18]	1.57/2.45/3.5	-	No	Microstrip line
[19]	1/2.55/3	3.7/4.2/4	No	Microstrip line
[20]	1/2.1/2.4	4/3.92/3.7	No	Microstrip line
This work	4.53/6.53/8.32	4.6/4.1/5.1	Yes	HMSIW

In this paper, the dual-band filtering power divider is designed by etching slots on the HMSIW cavity. The TE_{101} mode is perturbed, and the first center frequency is shifted slightly compared with Figure 2(b). To get good performance of S_{11} in the design of tri-band power divider, the sizes of slots and open-stub are optimized. The first center frequency and the second frequency of tri-band power divider are changed a little compared with dual-band power divider. In order to get operating frequencies, the sizes of cavity, slots and open-stub can be adjusted according to Figure 4 and Figure 8(a).

4. CONCLUSIONS

A compact tri-band filtering power divider based on HMSIW has been presented by analyzing the effects of the slots and open-stub on resonant frequencies. The third centre frequency is changed by adjusting the size of the open-stub without effect on the other two passbands. The presented circuit has been designed, fabricated and measured. A good agreement can be found between the simulated and measured results over the operating frequency range. This filtering HMSIW power divider can be widely used in microwave and millimeter-wave systems because of its simplicity, compactness and easy integration.

REFERENCES

1. Hui, J. N., W. J. Feng, and W. Q. Che, “Balun bandpass filter based on multilayer substrate integrated waveguide power divider,” *Electronics Letters*, Vol. 48, No. 10, 571–573, 2012.
2. Dang, T. S., C. W. Kim, and S. W. Yoon, “Ultra-wideband power divider using three parallel-coupled lines and one shunt stub,” *Electronics Letters*, Vol. 50, No. 2, 95–96, 2014.
3. Liu, H., C. Liu, and X. Dai, “Design of novel compact dual-band filtering power divider using stepped-impedance resonators with high selectivity,” *International Journal of RF and Microwave Computer-Aided Engineering*, Vol. 26, No. 3, 262–267, 2016.
4. Zhang, X. Y., K. X. Wang, and B. J. Hu, “Compact filtering power divider with enhanced second-harmonic suppression,” *IEEE Microwave & Wireless Components Letters*, Vol. 23, No. 9, 483–485, 2013.

5. Ren, X., K. Song, and B. Hu, "Compact filtering power divider with good frequency selectivity and wide stopband based on composite right-/left-handed transmission lines," *Microwave & Optical Technology Letters*, Vol. 56, No. 9, 2122–2125, 2014.
6. Ding, J., T. Zhang, and F. Liu, "Compact inline triplet SIW filter with embedded short-ended strip line," *Progress In Electromagnetics Research C*, Vol. 61, 127–130, 2016.
7. Hong, W., B. Liu, and Y. Wang, "Half mode substrate integrated waveguide: A new guided wave structure for microwave and millimeter wave application," *International Conference on Infrared Millimeter Waves and, International Conference on Terahertz Electronics*, 219–219, Irmmw-Thz, 2006.
8. He, Z., J. Cai, Z. Shao, X. Li, and Y. Huang, "A novel power divider integrated with SIW and DGS technology," *Progress In Electromagnetics Research*, Vol. 139, 289–301, 2013.
9. Chen, S. Y., D. S. Zhang, and Y. T. Yu, "Wideband SIW power divider with improved out-of-band rejection," *Electronics Letters*, Vol. 49, No. 15, 943–944, 2013.
10. Danaeian, M., A.-R. Moznebi, and K. Afrooz, "Miniaturised equal/unequal SIW power divider with bandpass response loaded by CSRRs," *Electronics Letters*, Vol. 52, No. 22, 1864–1866, 2016.
11. Chen, R. S., S. W. Wong, and L. Zhu, "Wideband bandpass filter using U-slotted substrate integrated waveguide (SIW) cavities," *IEEE Microwave & Wireless Components Letters*, Vol. 25, No. 1, 1–3, 2015.
12. Cheng, H. R., "Novel wideband bandpass filter integrating HMSIW with DGS," *Journal of Electromagnetic Waves & Applications*, Vol. 23, Nos. 14–15, 2031–2040, 2009.
13. Huang, T., C. Chang, and H. Chen, "Simple method for a K-band SIW filter with dual-mode quasi-elliptic function response," *Microwave & Optical Technology Letters*, Vol. 49, No. 6, 1246–1249, 2010.
14. Wong, S. W., K. Wang, and Z. N. Chen, "Electric coupling structure of substrate integrated waveguide (SIW) for the application of 140-GHz bandpass filter on LTCC," *IEEE Transactions on Components Packaging & Manufacturing Technology*, Vol. 4, No. 4, 316–322, 2014.
15. Zhang, X. Y., J. X. Chen, and Q. Xue, "Dual-band bandpass filters using stub-loaded resonators," *IEEE Microwave & Wireless Components Letters*, Vol. 17, No. 8, 583–585, 2007.
16. Wu, Y., J. Shen, and L. Liang, "A novel compact tri-band Wilkinson power divider based on coupled lines," *Electromagnetics*, Vol. 33, No. 1, 59–72, 2013.
17. Wang, X. H., Y. F. Bai, and H. Xu, "A tri-band Wilkinson power divider using step-impedance resonator," *IEEE Electrical Design of Advanced Packaging and Systems Symposium (EDAPS)*, 1–4, 2011.
18. Liu, W. Q., F. Wei, and X.-W. Shi, "A compact tri-band power divider based on triple-mode resonator," *Progress In Electromagnetics Research*, Vol. 138, 283–291, 2013.
19. Chu, Q. X., F. Lin, and Z. Lin, "Novel design method of tri-band power divider," *IEEE Microwave Theory & Techniques*, Vol. 5, No. 9, 2221–2226, 2011.
20. Hayati, M., S. A. Malakooti, and A. Abdipour, "A novel design of triple-band Gysel power divider," *IEEE Transactions on Microwave Theory & Techniques*, Vol. 61, No. 10, 3558–3567, 2013.